Pande, C., & Wishnia, A. (1986) *J. Biol. Chem. 261*, 6272–6278.
Peterson, J. (1971) *Arch. Biochem. Biophys. 144*, 678–693.
Poulos, T. L., Finzel, B. C., Gunsalus, I. C., Wagner, G. C., & Kraut, J. (1985) *J. Biol. Chem. 260*, 16122–16130.
Poulos, T. L., Finzel, B. C., & Howard, A. J. (1986) *Biochemistry 25*, 5314–5322.
Poulos, T. L., Finzel, B. C., & Howard, A. J. (1987) *J. Mol. Biol. 194*, 687–701.
Raag, R., & Poulos, T. L. (1989) *Biochemistry 28*, 917–922.
Satake, H., Imai, Y., Hashimoto, C., Sato, R., Shimizu, T., Nozawa, Y., & Hatano, M. (1976) *Seikagaku 48*, 508–510.
Sato, R., & Omura, T. (1978) in *Cytochrome P-450* (Ortiz de Montellano, Ed.) p 62, Academic Press, New York.
Schwarze, W., Blanck, J., Ristau, O., Jänig, G. R., Pommerening, K., Rein, H., & Ruckpaul, K. (1985) *Chem.-Biol. Interact. 54*, 127–141.
Sligar, S. G. (1976) *Biochemistry 15*, 5399–5406.
Sligar, S. G., & Gunsalus, I. C. (1976) *Proc. Natl. Acad. Sci. U.S.A. 73*, 1078.
Yu, C. A., & Gunsalus, I. C. (1974) *J. Biol. Chem. 249*, 102–106.

^{13}C NMR Relaxation Times of Hepatic Glycogen in Vitro and in Vivo†

Li-Hsin Zang,‡ Maren R. Laughlin,‡,§ Douglas L. Rothman,‖ and Robert G. Shulman*,‡
Department of Molecular Biophysics and Biochemistry and Department of Internal Medicine, School of Medicine, Yale University, New Haven, Connecticut 06510

Received January 30, 1990; Revised Manuscript Received April 20, 1990

ABSTRACT: The field dependence of relaxation times of the C-1 carbon of glycogen was studied in vitro by natural-abundance ^{13}C NMR. T_1 is strongly field dependent, while T_2 does not change significantly with magnetic field. T_1 and T_2 were also measured for rat hepatic glycogen enriched with [1-^{13}C]glucose in vivo at 4.7 T, and similar relaxation times were observed as those obtained in vitro at the same field. The in vitro values of T_1 were 65 ± 5 ms at 2.1 T, 142 ± 10 ms at 4.7 T, and 300 ± 10 ms at 8.4 T, while T_2 values were 6.7 ± 1 ms at 2.1 T, 9.4 ± 1 ms at 4.7 T, and 9.5 ± 1 ms at 8.4 T. Calculations based on the rigid-rotor nearest-neighbor model give qualitatively good agreement with the T_1 field dependence with a best-fit correlation time of 6.4×10^{-9} s, which is significantly smaller than τ_M, the estimated overall correlation time for the glycogen molecule (ca. 10^{-5} s). A more accurate fit of T_1 data using a modified Lipari and Szabo approach indicates that internal fast motions dominate the T_1 relaxation in glycogen. On the other hand, the T_2 relaxation is dominated by the overall correlation time τ_M while the internal motions are almost but not completely unrestricted.

Glycogen is the main storage form of glucose in mammalian cells. Although glycogen has a very high molecular weight (ca. 10^7) (Drochmans, 1962; Goldsmith et al., 1982), previous studies have shown that it is 100% ^{13}C NMR visible both in vitro and in vivo at ambient temperatures (Sillerud & Shulman, 1983; Hull et al., 1987; Shalwitz et al., 1987). This visibility has allowed many studies of synthesis and metabolism of glycogen in vivo by ^{13}C NMR spectroscopy (Jue et al., 1989; Laughlin et al., 1988; Reo et al., 1984; Shulman et al., 1988). Considering the high molecular weight, the estimated rotational correlation time (τ_M) for a rigid molecule with the size of glycogen would be ca. 10^{-5} s. This would lead to very short values of T_2, so that in the absence of any other motion the ^{13}C NMR lines of glycogen would be too broad to observe.

In order to understand the mechanism of NMR visibility of glycogen, we have studied the magnetic field dependence of the glycogen relaxation times in vitro. In addition, we have measured the T_1 and T_2 of hepatic glycogen directly in an intact living rat at 4.7 T. We have compared the experimental results with those of theoretical calculations based on the rigid-rotor nearest-neighbor model (RRNN)[1] and the modified Lipari and Szabo approach (MLSA).

Materials and Methods

In Vitro. Type III rabbit liver glycogen, prepared by hot water extraction, was purchased from Sigma Chemical Co. (St. Louis, MO). A solution of glycogen (30 mg/mL) in 50 mM phosphate buffer, pH 7, was prepared for natural-abundance ^{13}C NMR measurements at 2.1 and 4.7 T without further purification. For measurements at 8.4 T, D_2O was added to the solution to 10% by volume with a final glycogen concentration of 100 mg/mL.

Natural-abundance ^{13}C NMR measurements were performed on an 8.4-T Bruker Instrument AM superconducting spectrometer system, and on 2.1- and 4.7-T Biospec superconducting spectrometer systems, respectively. At 8.4 T, ^{13}C spectra of glycogen were taken at 90.5 MHz using a 5-mm probe. At 4.7 and 2.1 T, the spectra were taken at 50.4 and 22.89 MHz using 20-mm sample tubes in $^{13}C/^1H$ solenoidal probes. Spin–lattice relaxation times (T_1) and spin–spin relaxation times (T_2) were measured with the inversion recovery (180°–τ–90°) and spin-echo (90°–τ–180°–τ–echo) methods, respectively. Results were analyzed by using a three-parameter fitting program from the spectrometer computer (Bruker In-

† This work was supported by National Institutes of Health Grants DK27121 and GM30287.
‡ Department of Molecular Biophysics and Biochemistry.
§ Present address: National Heart Lung and Blood Institute, Lab of Myocardial Energetics, National Institutes of Health, Bethesda, MD 20892.
‖ Department of Internal Medicine.

[1] Abbreviations: MFA, model-free approach; MLSA, modified Lipari and Szabo approach; RRNN, rigid-rotor nearest-neighbor.

0006-2960/90/0429-6815$02.50/0

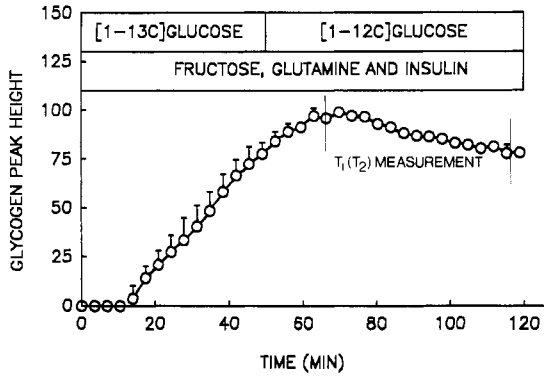

FIGURE 1: Peak intensity of hepatic [1-^{13}C]glycogen during the control experiment. A 50-min infusion of 10 mg/min [1-^{13}C]glucose, 5 mg/min fructose, 2 mg/min glutamine, and 20 milliunits/min insulin was followed by the same infusion containing unlabeled glucose for 70 min while sequential 3-min ^{13}C NMR spectra were collected. A relaxation measurement was started after ca. 20 min of unlabeled glucose infusion as marked in the figure.

strument, Billerica, MA) and NMR1 software (New Methods Research Inc., Syracuse, NY). For the relaxation time measurements, proton decoupling was gated on only during the acquisition, and a relaxation delay of 2 s was used between scans. Nuclear Overhauser enhancements (η + 1) were measured in proton-decoupled spectra obtained with the decoupler carrier frequency centered on the water resonance for 1.8 s ($\leq 5T_1$) before and during acquisition. A relaxation delay of 1.8 s without decoupling was used between pulses to prevent sample heating. Control spectra without NOE were acquired in exactly the same way except that the decoupler offset was moved 200 kHz from the water resonance during the NOE development period, and placed back on water during the acquisition. The η + 1 values were obtained from the ratio of the integrated NMR signal from the NOE spectrum and that from the corresponding control spectrum.

In Vivo. T_1, T_2, and NOE were measured for C-1 of glycogen in the livers of 300–400-g male Sprague-Dawley rats. They were fasted for 18–24 h and anesthetized with pentobarbital, and a catheter for substrate infusion was placed in a jugular vein. They were placed in the Bruker Biospec 4.7-T magnet with the abdomen positioned over a NMR probe that consisted of a 2-cm-diameter ^{13}C surface coil and a 3.8-cm-diameter ^{1}H coil arranged concentrically. The outer coil was used for shimming and proton decoupling; 3.5-min proton-decoupled (WALTZ-16) spectra consisting of 1000 scans were accumulated during the basal and infusion periods to monitor [1-^{13}C]glycogen signal intensity. The infusion consisted of 10 mg/min [1-^{13}C]glucose (99% enriched, MSD Isotopes, Montreal, Canada), 5 mg/min fructose, 2 mg/min glutamine, and 20 milliunits/min insulin. Once adequate signal-to-noise for [1-^{13}C]glycogen (100.6 ppm) was obtained, the [1-^{13}C]-glucose was replaced with unlabeled glucose and the infusion continued for the remainder of the experiment. T_1 inversion recovery measurements were started as soon as the C-1 glycogen signal in NMR spectra reached its plateau. Fully relaxed control spectra (720 scans) were taken immediately before and after the T_1 measurement. Corrections of the T_1 inversion recovery signals were done by assuming a linear decline of the glycogen C-1 signal intensity with respect to time (Laughlin et al., 1988). The change of the glycogen C-1 signal intensity during the experiment is illustrated in Figure 1. The complete spin inversion was achieved by an adiabatic fast-passage pulse (sech-shaped pulse) (Silver et al., 1985). After the short variable delay (τ), the depth pulses and the excitation pulse were followed. Composite proton decoupling (4 W) was gated on during the acquisition, and a relaxation delay of 0.8 s was used between scans.

Table I: Experimental Relaxation Data of Glycogen C-1

B_0 (T)	temp (K)	T_1 (ms)	T_2 (ms)	$(\pi\Delta\nu_{1/2})^{-1}$ (ms)[a]	η + 1
2.1	295	65 ± 5	6.7 ± 1	8.8 ± 1	1.32
4.7	295	142 ± 10	9.4 ± 1	7.8 ± 1	1.30
	in vivo ($T \approx 310$ K)	158 ± 15	5 ± 2	8 ± 3	1.35
8.4	295	300 ± 10	9.5 ± 1	8.5 ± 1	1.22
	300	300 ± 10	14 ± 2	8.5 ± 1	1.31
	310	310 ± 10	13 ± 2	11 ± 1	1.41

[a] $\Delta\nu_{1/2}$ was obtained by subtracting the B_0 inhomogeneity and the line broadening from the observed full width at half-maximum.

The same preparation and infusion procedures were used for the T_2 measurement. The pulse sequence used in the spin-echo measurement was (relaxation delay)–2θ–τ–(depth pulses)–θ–τ–echo, and composite proton decoupling was gated on during acquisition of the echo. Measurements at 6 τ values, with 720 scans each, were taken. NOE was measured in continuous proton-decoupled spectra, and the control spectra were taken with proton decoupling gated on only during acquisition.

In vivo ^{13}C NMR line widths were determined by fitting the fully relaxed signals to a single Lorentzian function using the fitting program in the spectrometer computer. The natural line width of the glycogen C-1 was then obtained by subtracting the field inhomogeneity and the line broadening. T_2^* was calculated from the natural line width and compared with the measured T_2.

Theoretical Calculations. For ^{13}C NMR of a protonated carbon, such as the C-1 of glycogen, the relaxation mechanism is primarily dipolar interactions. The relaxation times are given by

$$1/T_1 = (\hbar^2\gamma_C^2\gamma_H^2/4r_{CH}^6)[J(\omega_H - \omega_C) + 3J(\omega_C) + 6J(\omega_H + \omega_C)] \quad (1)$$

$$1/T_2 = (\hbar^2\gamma_C^2\gamma_H^2/8r_{CH}^6) \times [4J(0) + J(\omega_H - \omega_C) + 3J(\omega_C) + 6J(\omega_H) + 6J(\omega_H + \omega_C)] \quad (2)$$

where ω_C and ω_H are the Larmor frequencies for carbon and proton, respectively. r_{CH} is the distance of the C–H bond, and $J(\omega)$ is the spectral density function. In order to calculate the $J(\omega)$ terms, we first used the simplest approximation, the rigid-rotor nearest-neighbor model (RRNN), assuming the existence of a single effective correlation time. For a more flexible theoretical calculation, we adapted Lipari and Szabo's (1982) model-free approach (MFA), since the overall motion of a glycogen molecule is expected to be much slower than the internal motions. In addition, we used a χ^2 distribution of the correlation times to describe the internal motions of the glycogen molecule, and the corresponding $J(\omega)$ was solved numerically using computer programs. These theoretical treatments will be discussed in detail in the later section.

Results and Discussion

Experimental Data. The in vivo inversion recovery measurement of glycogen in the intact rat liver is shown in Figure 2. The figure shows the good NMR signal-to-noise ratio of the glycogen C-1 signal and the complete inversion of the spins in the sampled volume by the adiabatic pulse. The C-1 NMR signals observed both in vivo (shown in the insert of Figure 2) and in vitro can be fitted with a single Lorentzian function. T_1, T_2, T_2^*, and NOE data obtained in vitro and in vivo are summarized in Table I. Results obtained at three different

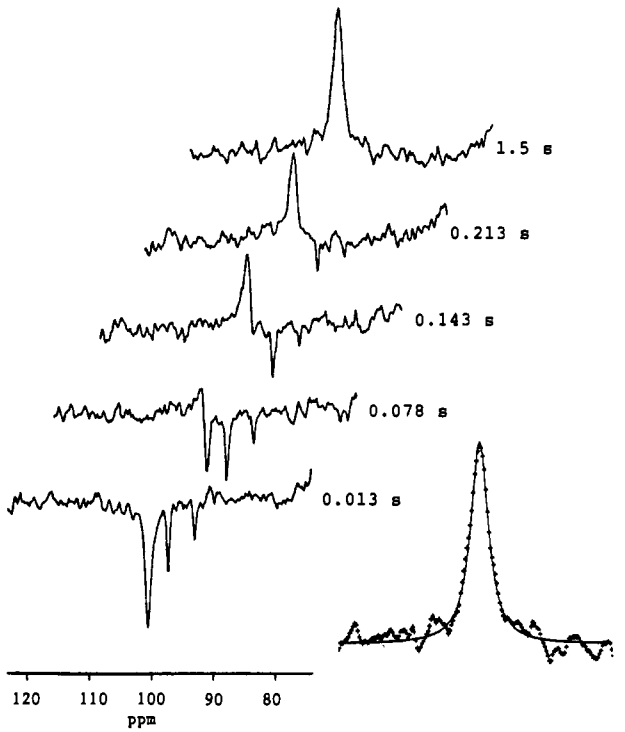

FIGURE 2: In vivo inversion recovery measurement of [1-^{13}C]glycogen in a rat liver at the five values of variable delay (τ) labeled. See Materials and Methods for the experimental conditions and procedures. A total of 720 scans with a relaxation delay of 0.8 s were accumulated for each spectrum. The entire measurement took about 45 min. The insert shows the in vivo glycogen C-1 signal (with 40-Hz line broadening) fit to a single Lorentzian function.

temperatures at 8.4 T show that the T_1 does not change significantly. However, small but significant changes in T_2, T_2*, and NOE were detected. The results show that the T_1 of glycogen in solution exhibits a strong field dependency, while T_2 does not vary significantly with the field. Furthermore, the relaxation times and the NOE factor of glycogen C-1 in the rat liver measured at 4.7 T in vivo are similar to those of glycogen in solution measured at the same field strength. These similarities suggest that the molecular motions and the effective correlation times of glycogen in vivo are the same as those in vitro. Therefore, a similar field dependency of T_1 in vivo is expected, but the measurements have not been made. The T_2 value obtained from in vivo measurements is smaller than that obtained in solution at 4.7 T (Table I). The difference may be originated from the slower overall motion of glycogen particles in vivo. We will show in a later section that T_2 is very sensitive to the overall rotational correlation time of the particle, while T_1 is not. On the other hand, the in vivo T_2* value reported in Table I may contain large uncertainties because the natural line width is obtained by subtracting a large contribution of the B_0 inhomogeneity (21 Hz) and the line broadening (40 Hz) from the observed signal line width (98 Hz), which drastically reduces the natural line width to 37 Hz. Furthermore, the B_0 inhomogeneity in vivo is estimated from the water line width (84 Hz) obtained by the outer ^{1}H decoupling coil which may lead to an overestimation of B_0 inhomogeneity on carbon signals. Therefore, T_2* is probably overestimated since it is impossible to have T_2* > T_2.

Electron microscopic studies have shown that glycogen particles are made of spherical units with an average radius of 20 nm (Wanson & Drochmans, 1968). The overall rotational correlation time of a spherical particle can be estimated by the Stokes relation $\tau_M = (4\pi\eta)r_s^3/3kT$, where k is Boltzmann's constant, T is the absolute temperature, η is the viscosity, and r_s is the Stokes radius. When r_s = 20 nm and η = 0.1 cP, τ_M is estimated to be 8.2 × 10^{-6} s at 300 K. The strong field dependence of T_1 observed in vitro indicates that the effective correlation time of glycogen relaxation, τ_c, is not in the "extreme narrow limit" region. On the other hand, values obtained for T_2 suggest that this correlation time is much shorter than the molecular rotation time τ_M. In order to determine the effective correlation time of glycogen, we first fit the data to the RRNN model.

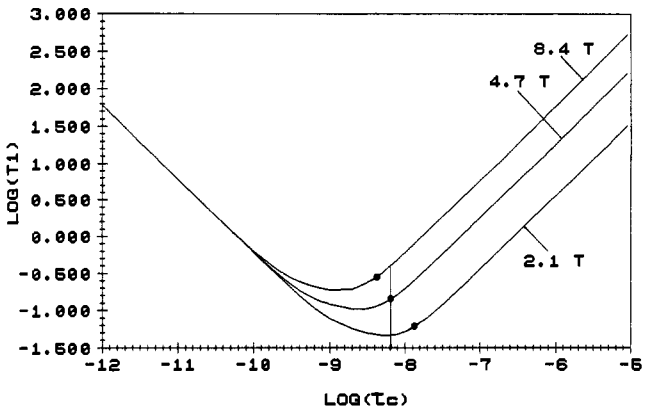

FIGURE 3: Log-scaled plot of glycogen T_1 vs correlation time (τ_c) at three field strengths, calculated from the RRNN model (see text). The experimental T_1 data (●) are shown on the curves, and an approximate fit gives τ_c = 6 × 10^{-9} s (as marked).

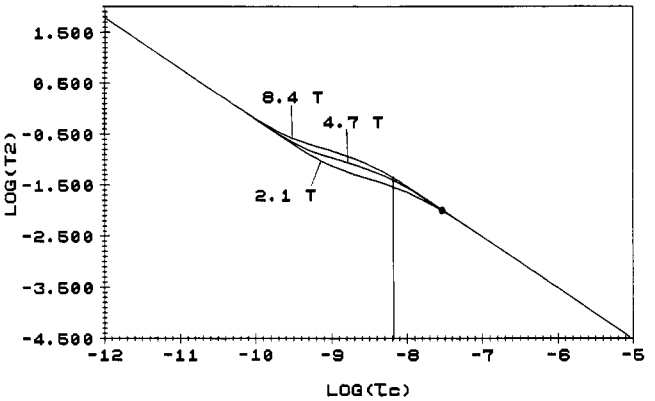

FIGURE 4: Log-scaled plot of glycogen T_2 vs correlation time τ_c at three field strengths, calculated from the RRNN model (see text). The experimental T_2 data (●) are shown on the curves. The average correlation time obtained from T_1 fitting (6 × 10^{-9} s) is marked on the plot.

RRNN Model. As shown in eq 1 and 2, to calculate T_1 and T_2, one needs to evaluate the $J(\omega)$ and $J(0)$ terms, where $J(\omega)$ is defined by

$$J(\omega) = 2\int_0^\infty (\cos \omega t)C(t)\, dt \qquad (3)$$

$C(t)$ is the correlation function of the system. Generally, specific models are needed to define correlation functions. In the RRNN model, the correlation function is described as a single exponential function with a lifetime of τ_c:

$$C(t) = (1/5)\exp(-t/\tau_c) \qquad (4)$$

Therefore, the corresponding $J(\omega)$ term can be written as

$$J(\omega) = (2/5)[\tau_c/(1 + \omega^2\tau_c^2)] \qquad (5)$$

Assuming that glycogen relaxation can be described with a single effective correlation time (τ_c), we calculated T_1 and T_2 at different correlation times using the RRNN model at the three field strengths we studied. Figures 3 and 4 show the log-scaled plots of T_1 and T_2 vs τ_c times, respectively. In the

Table II: Experimental Relaxation Data of Glycogen C-1 and Results Calculated from the RRNN Model and the Modified Lipari and Szabo Approach

B_0 (T)	temp (K)	T_1^{exp} (ms)	T_1^{RRNN} (ms)[a]	T_1^{MLSA} (ms)[b]	T_2^{exp} (ms)	T_2^{RRNN} (ms)[a]	T_2^{MLSA} (ms)[b]
2.1	295	65 ± 5	46.4	63.4	6.7 ± 1	29.4	8.79
4.7	295	142 ± 10	141.6	148.5	9.4 ± 1	40.0	9.29
8.4	295	300 ± 10	401.8	300.5	9.5 ± 1	44.6	9.49

[a] Calculated by using the RRNN model with a correlation time of $\tau_c = 6.4 \times 10^{-9}$ s and $r_{CH} = 1.14$ Å (see text). [b] Calculated by using MLSA with $\tau_M = 8.23 \times 10^{-6}$ s, $\tau_{av} = 3.9 \times 10^{-9}$ s, and $S^2 = 0.0022$ (see text).

calculation, we took r_{CH} to be 1.14 Å (Brown, 1984) and assumed that this was the only dipolar interaction. Comparison of the experimental and calculated T_1 values shows that although the T_1 data cannot be fitted with a single correlation time exactly, the average τ_c of 6.4×10^{-9} s fits all the data approximately and is obviously much smaller than τ_M. This indicates that the internal motions of glycogen, characterized with a much shorter correlation time τ_c, play an important role in the T_1 relaxation. The calculated results are shown in Table II. A weak field dependency calculated for T_2 (Figure 4) is consistent with that observed experimentally. However, the T_2 values calculated by using $\tau_c = 6.4 \times 10^{-9}$ s in the RRNN model are 4–5 times larger than those measured experimentally. The T_2 data would be better fitted by using a longer τ_c of ca. 3×10^{-8} s, suggesting that slower motions may contribute to the T_2 relaxation of glycogen.

Modified Lipari and Szabo Approach (MLSA). In order to obtain a more accurate description for the observed relaxation times, we used Lipari and Szabo's model-free approach for the following reasons. First, the overall motion of glycogen is much slower than the internal motions, as shown in the RRNN treatment. Therefore, the overall motion can be rigorously factored out and treated independently, which is a basic assumption in the MFA. Second, the precise description of the correlation function for the internal motions of a macromolecule depends on a model. It is complicated and difficult to establish a model to describe the motion of a ^{13}C–H vector in a glycogen molecule which has a highly complex structure. The MFA avoids this requirement by introducing a generalized order parameter, S, and an effective correlation time, τ_e, to describe the spatial restriction of the motion and the rate of the motion, respectively.

According to the MFA, the correlation function of glycogen, $C(t)$, is defined as

$$C(t) = C_o(t)C_I(t) \quad (6)$$

where $C_o(t)$ and $C_I(t)$ are correlation functions for the overall and the internal motions, respectively. Since the glycogen particle is roughly spherical, we assume that its overall motion is isotropic and can be described with a single correlation time, τ_M. Hence

$$C_o(t) = (1/5)\exp(-t/\tau_M) \quad (7)$$

The correlation function for the internal motions is given by

$$C_I(t) = \sum_{i=0}^{\infty} a_i \exp(-t/\tau_i) = S^2 + \sum_{i=1}^{\infty} a_i \exp(-t/\tau_i) \quad (8)$$

where S ($S^2 = a_0$) is the generalized order parameter. The combination of eq 7 and 8 gives the total correlation function, and the corresponding spectral density function is

$$J(\omega) = (2/5)[S^2\tau_M/(1 + \omega^2\tau_M^2)] + (2/5)\sum_{i=1}^{\infty}[a_i\tau_i/(1 + \omega^2\tau_i^2)] \quad (9)$$

In the MFA, assuming the internal motions are in the extreme narrowing limit and the summation term can be evaluated by a single exponential term with an effective correlation time τ_e (Lipari & Szabo, 1982), eq 9 is simplified to

$$J(\omega) = (2/5)[S^2\tau_M/(1 + \omega^2\tau_M^2) + (1 - S^2)\tau_e] \quad (10)$$

which is Lipari and Szabo's eq 36. Unfortunately, the simplified equation cannot be used in the case of glycogen. Although the internal motions are much faster than the overall motion, the average correlation time of internal motions is not in the extreme narrowing limit region, as shown by the RRNN calculation. In an attempt to evaluate the second term in eq 9 (the internal motion part), we adapted the method of using a distribution of correlation times, which has been applied to random-coiled polymers to describe segmental motions (Schaefer, 1973), since glycogen is a large and highly branched monopolymer. Therefore, $J(\omega)$ can be written as

$$J(\omega) = (2/5)[S^2\tau_M/(1 + \omega^2\tau_M^2)] + (2/5)J_I(\omega) \quad (11)$$

$$J(0) = (2/5)[S^2\tau_M + J_I(0)] \quad (12)$$

where

$$J_I(\omega) = \int_0^{\infty} p(\tau_r)\tau_{av}\tau_r/[1 + \omega^2(\tau_{av}\tau_r)^2]\, d\tau_r \quad (13)$$

and $p(\tau_r)$ is a distribution density function. τ_r is the reduced correlation time, which is defined by

$$\tau_r = \tau_i/\tau_{av}$$

According to Schaefer (1973), based on an assumption that the slow motiions have a higher density than the very fast ones, the log-scaled (log of b base) χ^2 distribution of time can be used, and assuming $\tau_M \gg \tau_i$ under the distribution and $S^2 \ll 1$, the $J_I(\omega)$ of glycogen (eq 13) can be written as

$$J_I(\omega) = \int_0^{\infty} \frac{\tau_{av}p^{(n)}(s)(b^s - 1)\, ds}{(b-1)\{1 + \omega^2\tau_{av}^2[(b^s - 1)/(b-1)]^2\}} \quad (14)$$

and

$$J_I(0) = \int_0^{\infty} \frac{\tau_{av}p^{(n)}(s)(b^s - 1)\, ds}{b - 1} \quad (15)$$

where the χ^2 distribution, $p^{(n)}(s)$, is defined as

$$p^{(n)}(s)\, ds = \frac{1}{\Gamma(n)}(ns)^{n-1}e^{-ns}n\, ds \quad (16)$$

and

$$s = \log_b[1 + (b-1)\tau_i/\tau_{av}]$$

The distribution is normalized to unity:

$$\int_0^{\infty} p^{(n)}(s)\, ds = 1 - S^2 \approx 1 (S^2 \ll 1) \quad (17)$$

In our calculations, $J_I(\omega)$ and $J_I(0)$ terms were numerically evaluated by using computer programs. By using eq 15, 14, 12, 11, 2, and 1, we can calculate T_1 and T_2 for any given τ_{av}, providing the correlation time of the overall motion τ_M, the generalized order parameter S, and the order of the distribution (b, n) are given. Figure 5 shows the log-scaled plot of T_1 vs the averaged correlation time of the internal motions τ_{av} calculated by the MFA with the distribution method. The

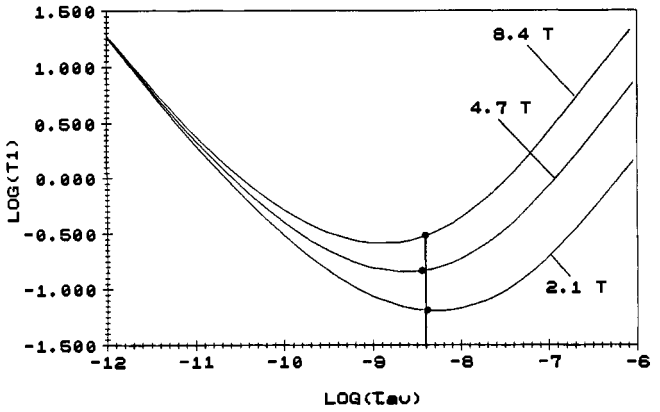

FIGURE 5: Log-scaled plot of glycogen T_1 vs average correlation time τ_{av} at three field strengths, calculated from MLSA with a χ^2 distribution of correlation times of the internal motions (see text). For the distribution function (see Figure 6), $n = 21$ and $b = 600$. $r_{CH} = 1.14$ Å. The fit of experimental T_1 data [labeled by (●)] gives $\tau_{av} = 3.9 \times 10^{-9}$ s.

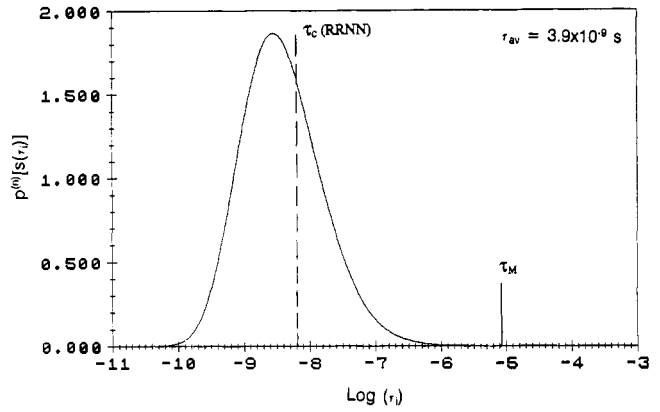

FIGURE 6: Plot of χ^2 distribution density vs log τ_i. In eq 16, $n = 21$ and $b = 600$; $\tau_{av} = 3.9 \times 10^{-9}$ s. The τ_i values at half-maximum are 6.58×10^{-8} and 1.65×10^{-10} s. τ_c obtained from the RRNN calculation is shown by (- - -), and the τ_M of glycogen is shown by (—).

distribution that gives the best T_1 and T_2 fitting, having $\tau_{av} = 3.9 \times 10^{-9}$ s, is shown in Figure 6. The values of τ_i at half-maximum are 6.58×10^{-10} and 1.65×10^{-8} s. As shown in Figure 5, the distribution line width of the internal motions is rather narrow, and all τ_i values are indeed much smaller than τ_M, which suggests that the internal motions of C-1 throughout glycogen are rather uniform. The calculated values based on the MLSA and the RRNN model are summarized in Table II along with the experimental results. The comparison shows that results obtained by the MLSA calculation give a better fit to the data than those obtained by the RRNN model, as expected from the additional degrees of freedom.

The calculations based on the MLSA show that S^2 has almost no effect on T_1 at the field strengths we studied, as long as S^2 is smaller than 0.1. This is due to the fact that τ_M is very long so that $\omega^2\tau_M^2 \gg 1$, which makes the first term in eq 11 negligible compared to the second term when τ_{av} is between 10^{-9} and 10^{-8} s. It is consistent with the results obtained by the RRNN model in which the contribution from the overall motion is neglected. However, the situation is completely different for T_2 because of its dependence on the $J(0)$ term. In fact, we have turned to the MLSA because the RRNN model does not calculate values of T_2 that agree with experimental values so that we must try to find an additional contribution to T_2 relaxation. Since $J(0)$ is proportional to the overall correlation time, τ_M, which is much larger than the average internal correlation time τ_{av}, it can be a dominant factor in determining T_2 even if S^2 is small. Therefore, the amplitude of T_2 is sensitive to the $S^2\tau_M$ value, and in fact, S^2 reported in Table II is obtained from fitting T_2 to eq 12 with the value of τ_M fixed. According to Lipari and Szabo, if the internal motion is completely restricted, then $S^2 = 1$; if the motion is isotropic (completely unrestricted), $S^2 = 0$. It is not unexpected that S^2 is very small ($S^2 = 0.0022$) if we compare the experimental data with those calculated by using the RRNN model. Without taking account of the overall motion of glycogen, the T_2 results obtained from the RRNN model by taking $\tau_c = 6.4 \times 10^{-9}$ s are several times larger than those obtained experimentally (Table II). Although the contribution from the overall motion to T_1 is negligible, it cannot be neglected in the T_2 calculations where it makes a dominant contribution due to the dependence of the $J(0)$ term. Furthermore, the measured temperature dependence of T_2 but not of T_1 (Table I) may result from the determination of T_2 by τ_M and S^2, which may be more sensitive to temperature than τ_{av}. We have noted that T_2 measured in vivo is about half of that in solution at 4.7 T. The 2-fold smaller value of T_2 in vivo might come from slower tumbling of the glycogen molecule in vivo since an increase in rotational correlation time by a factor of 2, which has often been measured in vivo (Beall, 1983), would explain the observed value of T_2. Obviously, more work must be done on T_2 and T_2^* measurements in vivo.

Comparison with Polysaccharides. ^{13}C NMR has been widely used to determine molecular motions of mono-, oligo-, and polysaccharides [see Casu (1985) and references cited therein]. Many polysaccharides studied yield high-resolution ^{13}C NMR spectra, due to rapid internal isotropic molecular tumbling. However, signal broadening has been observed in the less mobilized segments involved in junction zones. Studies of curdlan, a β-1,3-glucan (Saito et al., 1977, 1978) have shown that ^{13}C NMR signals become partially invisible upon formation of gel structure. However, the fraction which remained visible had approximately the same T_1 as for the solubilized polymer which was 100% visible. Similar to our calculation of internal motions of glycogen, Smith and Saito (1980) treated the relaxation data of curdlan with the ln χ^2 distribution method (Schaefer, 1973). Their results show that the average correlation times are 30–40 ns for the gel-formed sample (dp_n 540) and 4.3–22 ns for the random-coiled sample which shows 100% visibility. Furthermore, the width of the distribution for the gel-state molecular motions is much greater. The authors concluded from these studies that provided the polymer is in the single-coil conformation the internal motions are rapid enough to make it 100% visible even at chain lengths of over 300 and immobilized in a gel. The invisible fraction was attributed to segments involved in cross-chain interactions which restricted the internal motion. In glycogen, the average correlation time for the internal motions is ca. 10 times smaller than for curdlan, and the distribution width is narrow, indicating a large degree of flexibility is rather uniformly distributed to the entire molecule. In contrast to polysaccharides, polyglucose chains in glycogen are not very long (12–14 residues per chain) due to its frequent branching, although it has a very high molecular weight. In addition, the 100% visibility suggests, on the basis of the data on curdlan and other gel-forming polysaccharides, that there is no significant binding interaction between the chains in the glycogen molecule.

In conclusion, measurements of relaxation times of glycogen ^{13}C-1 in vitro at different field strengths show that T_1 is strongly field dependent, while T_2 is only weakly field dependent. The relaxation measurements obtained from an intact rat liver further demonstrate that T_1 and T_2 of glycogen

C-1 in vivo are similar to those observed in vitro. These relaxation properties can only be approximately fitted by the RRNN model calculation using a single effective correlation time τ_c. However, the strong field dependence of T_1 and the absolute values of T_2 are not adequately explained by this model. The MLSA calculation provides a much better fit to the relaxation times and accordingly gives more information about motions of the glycogen molecule. The results suggest that internal motions dominate the relaxation with an average correlation time of 3.9×10^{-9} s. The fit to the T_2 data shows that the overall molecular tumbling makes the strongest contribution to the T_2 relaxation but it is much less than expected from a rigid molecule, once again showing that the internal motions of glycogen are almost unrestricted throughout the molecule. This particular molecular nature of glycogen leads to the observation of narrow ^{13}C resonances which leads to the 100% ^{13}C NMR visibility.

References

Beall, P. T. (1983) *Cryobiology 20*, 324-334.

Brown, M. F. (1984) *J. Chem. Phys. 80*, 2832-2836.

Casu, B. (1985) *Top. Mol. Struct. Biol. 8*, 1-40.

Drochmans, P. (1962) *J. Ultrastruct. Res. 6*, 141.

Goldsmith, E., Sprang, S., & Fletterick, R. (1982) *J. Mol. Biol. 156*, 411-427.

Hull, W. E., Zerfowski, M., & Bannasch, P. (1987) *Proc. Magn. Reson. Med.*, 488.

Jue, T., Rothman, D. L., Tavitian, B. A., & Shulman, R. G. (1989) *Proc. Natl. Acad. Sci. U.S.A. 86*, 1439-1442.

Laughlin, M. R., Petit, W. A., Jr., Dizon, J. M., Shulman, R. G., & Barrett, E. J. (1988) *J. Biol. Chem. 263*, 2285-2291.

Lipari, G., & Szabo, A. (1982) *J. Am. Chem. Soc. 104*, 4546-4570.

Reo, N. V., Siegfried, B. A., & Ackerman, J. J. H. (1984) *J. Biol. Chem. 259*, 13664-13667.

Saito, H., Ohki, T., & Sasaki, T. (1977) *Biochemistry 16*, 908-914.

Saito, H., Miyata, E., & Sasaki, J. (1978) *Macromolecules 11*, 1244-1251.

Schaefer, J. (1973) *Macromolecules 6* (6), 882-888.

Shalwitz, R. A., Reo, N. V., Becker, N. N., & Ackerman, J. J. H. (1987) *Magn. Reson. Med. 5*, 462-465.

Shulman, G. I., Rothman, D. L., Chung, Y., Rossetti, L., Petit, W. A., Jr., Barrett, E. J., & Shulman, R. G. (1988) *J. Biol. Chem. 263*, 5027-5029.

Sillerud, L. O., & Shulman, R. G. (1983) *Biochemistry 22*, 1087-1094.

Silver, M. S., Joseph, R. I., & Hoult, D. I. (1985) *Phys. Rev. A31*, 2753.

Smith, I. C. P., & Saito, H. (1980) *Int. Congr. Pure Appl. Chem. 27th*, 213-223.

Wanson, J. J., & Drochmans, P. (1968) *J. Cell Biol. 38*, 130-150.

(Difluoromethylene)phosphates of Guanine Nucleosides as Probes of DNA Polymerases and G Proteins†

Lili Arabshahi,‡ Naseema N. Khan, Michelle Butler, Timothy Noonan, Neal C. Brown, and George E. Wright*

Department of Pharmacology, University of Massachusetts Medical School, Worcester, Massachusetts 01655

Received February 22, 1990; Revised Manuscript Received April 17, 1990

ABSTRACT: 5′-Polyphosphates of N^2-(*p*-*n*-butylphenyl)-2′-deoxyguanosine and -guanosine which contain a difluoromethylene group in place of a phosphoanhydride oxygen have been synthesized. 5′-[β,γ-(Difluoromethylene)triphosphates], including that of 2′-deoxyguanosine, were prepared by reaction of the corresponding 5′-phosphates, activated by 1,1′-carbonyldiimidazole, with difluoromethanediphosphonate. The 5′-[(difluoromethylene)diphosphate] of N^2-(*p*-*n*-butylphenyl)guanosine was prepared by treatment of a protected 5′-tosyl nucleoside with difluoromethanediphosphonate, followed by deprotection. Condensation of this nucleotide, activated with 1,1′-carbonyldiimidazole, with orthophosphate gave N^2-(*p*-*n*-butylphenyl)guanosine 5′-[(α,β-difluoromethylene)triphosphate]. Products were characterized by ^{31}P and ^{19}F NMR spectroscopy. The phosphonates were tested for their ability to displace [^{3}H]GDP from the GTP binding proteins cellular (EC) and oncogenic (Leu-61) Ha-*ras* p21, and for their ability to inhibit DNA polymerase α from Chinese hamster ovary cells. The p21s bound weakly to a triphosphonate when the CF_2 group was in the β,γ position, but not when it was in the α,β position, and they did not bind to the corresponding (difluoromethylene)diphosphate. In contrast, the CF_2 group had no effect on inhibition of DNA polymerase α by N^2-(*p*-*n*-butylphenyl)-2′-deoxyguanosine 5′-[(β,γ-difluoromethylene)triphosphate]. 2′-Deoxyguanosine 5′-[(β,γ-difluoromethylene)triphosphate] was found to be a bona fide substrate for several DNA polymerases and had a lower apparent K_m than dGTP with *Bacillus subtilis* DNA polymerase III.

Direct study of nucleoside triphosphate bound forms of DNA polymerases and G proteins is limited by the ability of the proteins to alter the structure of the nucleotides. DNA polymerases in the presence of template-primers incorporate many dNTP derivatives with the release of pyrophosphate, and the GTPase activity of G proteins degrades GTP derivatives to the nucleoside 5′-diphosphate and orthophosphate. Numerous studies [see, for example, Burgers and Eckstein (1979), Blackburn et al. (1985), and Tucker et al. (1986)] have explored effects of modification of the triphosphate group of nucleotides to determine the electronic and stereochemical requirements for binding to relevant proteins, and to identify, among candidate analogues, those that might serve as stable

† This research was supported by NIH Grants GM21747 to G.E.W. and CA40893 to N.C.B.

* Author to whom correspondence should be addressed.

‡ Current address: Cambridge Bioscience Corp., 365 Plantation Street, Worcester, MA 01655.

0006-2960/90/0429-6820$02.50/0